International Journal of Heat and Fluid Flow 30 (2009) 706–714

Contents lists available at ScienceDirect

International Journal of Heat and Fluid Flow

journal homepage: www.elsevier.com/locate/ijhff

Investigating the diameter of solid particles effects on a laminar nanofluid flow in a curved tube using a two phase approach

A. Akbarinia [a,b,*], R. Laur [b]

[a] New Energies Dept., Energy Research Institute, International Center for Science, High Technology & Environmental Sciences, Mahan, Iran
[b] Institute for Electromagnetic Theory and Microelectronics (ITEM), University of Bremen, Bremen, Germany

ARTICLE INFO

Article history:
Received 6 November 2007
Received in revised form 4 December 2008
Accepted 9 March 2009
Available online 5 April 2009

Keywords:
Nanofluid
Two phase
Curved tube
Laminar

ABSTRACT

In this paper, we report the results of our numerical studies on laminar mixed convection heat transfer in a circular Curved tube with a nanofluid consisting of water and 1 vol.% Al_2O_3. Three dimensional elliptic governing equations have been used. Two phase mixture model and control volume technique have been implemented to study flow field. Effects of the diameter of particles on the hydrodynamic and thermal parameters are investigated and discussed. Increasing the solid particles diameter decreases the Nusselt number and secondary flow, while the axial velocity augments. When the particles are in order of nano meter, increasing the diameter of particles, do not change the flow behaviors. The distribution of solid nanoparticles is uniform and constant in curved tube.

1. Introduction

In recent years, modern technologies have permitted the manufacturing of metallic particles down to the nanometer scale, which in turn created a new class of fluids, called nanofluids. This term refers to a two phase mixture that is usually composed of a saturated liquid and extremely fine metallic particles (40 nm or smaller) called nanoparticles.

It has been known that the thermal conductivity of these nanofluids is considerably higher than that of the base fluid (Masuda et al., 1993; Choi, 1995; Lee et al., 1999). The nanofluids constitute a very interesting alternative for advanced thermal applications, in particular in micro and nano scale heat transfer where a high heat flux is required (Lee and Choi, 2000). In spite of their interesting potential and features, these rather special fluids are still in their early development stage. The very first and scarce experimental works were mostly concerned with the measurement of the nanofluids effective thermal conductivity and dynamic viscosity (Masuda et al., 1993; Choi, 1995; Lee et al., 1999; Pak and Cho, 1998; Wang et al., 1999; Eastman et al., 1999, 2001; Xuan and Li, 2000). Das et al. (2003) and Putra et al. (2003) were likely the first who investigated the influence of temperature on nanofluid thermal properties. Their measurements for a water–Al_2O_3 mixture, although limited to two particular particle concentrations (e.g. 1% and 4%), have clearly shown that with an increase of temperature the effective thermal conductivity augments considerably. On the other hand the dynamic viscosity decreases appreciably, which is quite interesting for potential uses of nanofluids in various thermal applications. The experimental works by Pak and Cho (1998), Li and Xuan (2002) and Wen and Ding (2004) have provided interesting insights into the hydrodynamic and thermal behavior of nanofluids in confined flows and have confirmed their superior thermal performance. These results led to the first empirical Nusselt number correlations for both laminar and turbulent tube flow of nanofluids composed of water and metallic particles such as Cu, TiO_2 and cAl_2O_3. In their most recent work, Yang et al. (2005) have measured the convective heat transfer coefficients of several nanofluids composed of graphitic nanoparticles and automatic transmission fluid. Results from these pioneer works have clearly shown that the inclusion of dispersed particles produces a remarkable increase of the heat transfer flux since the convective heat transfer coefficient of the nanofluids for a given Reynolds is, in general, considerably higher than the corresponding one for the base fluid (saturated water). This improvement increases with an augmentation of the particle loading.

Numerous theoretical and experimental studies have been conducted to determine the effective thermal conductivity of nanofluids. Most of these have been confined to liquids containing micro and milli-sized suspended solid particles. However, studies show that the measured thermal conductivity of nanofluids is much larger than the theoretical predictions (Choi et al., 2001). Many attempts have been made to formulate efficient theoretical models for the prediction of the effective thermal conductivity,

* Corresponding author. Address: New Energies Dept., Energy Research Institute, International Center for Science, High Technology & Environmental Sciences, Mahan, Iran. Tel.: +49 421 2183462; fax: +49 421 2184434.
E-mail address: a.akbarinia@item.uni-bremen.de (A. Akbarinia).

0142-727X/$ - see front matter © 2009 Elsevier Inc. All rights reserved.
doi:10.1016/j.ijheatfluidflow.2009.03.002

Nomenclature

a	radius of curved pipe (m)
a	acceleration (ms^{-2})
C_p	specific heat (J/kg K)
d	horizontal direction
D	diameter of curved tube (m)
De	Dean number ($=Re\cdot\delta^{1/2}$)
f_θ	local skin friction coefficient
g	gravitational acceleration ($m\,s^{-2}$)
Gr	Grashof number ($=\frac{g\beta_m q'' D^4}{k_m \upsilon_m^2}$)
Nu_θ	local Nusselt number ($=\frac{q'' D}{k_m (T_w - T_b)}$)
P	pressure (pa)
Pr	Prandtl number ($=\frac{\alpha_m}{\nu_m}$)
q''	uniform heat flux ($W\,m^{-2}$)
R_c	curvature radius
Re	Reynolds number ($=\frac{\rho_m V_0 D}{\mu_m}$)
T	temperature (k)
V	velocity ($m\,s^{-1}$)
y	vertical direction

Greek symbols

α	thermal diffusivity
β	volumetric expansion coefficient (K^{-1})
δ	curvature ratio ($=a/R_c$)
λ	thermal conductivity (W/m K)
θ	angular coordinate in axial direction
ϕ	volume fraction
μ	dynamic viscosity ($N\,s\,m^{-2}$)
ν	kinematics viscosity ($m^{-2}\,s^{-1}$)
ρ	density ($kg\,m^{-3}$)

Subscripts

0	inlet condition
b	bulk
f	base fluid
m	mixture
p	particle
r	radial direction
s	solid phase
w	wall
z	axial direction
φ	tangential direction

but there is still a serious lack in this domain (Xue, 2003; Xuan et al., 2003).

Convective heat transfer with nanofluids can be modeled using the two phase or single phase approach. The first provides the possibility of understanding the functions of both the fluid phase and the solid particles in the heat transfer process. The second assumes that the fluid phase and particles are in thermal equilibrium and move with the same velocity. This approach is simpler and requires less computational time. Thus it has been used in several theoretical studies of convective heat transfer with nanofluids (Maige et al., 2004a,b; Roy et al., 2004; Khanfar et al., 2003; Akbarinia and Behzadmehr, 2007; Akbarinia, 2008). However, due to the fact that the effective properties of nanofluids are not known precisely, the numerical predictions of this approach are, in general, not in good agreement with experimental results. Therefore, the concerns in single phase modeling consist in selecting the proper effective properties for nanofluids and taking into account the chaotic movement of ultra fine particles. To partially overcome this difficulty, some researchers (for instance, Xuan and Li, 2000; Xuan and Roetzel, 2000) have used the dispersion model which takes into account the improvement of heat transfer due to the random movement of particles in the main flow. Recently Behzadmehr et al.(2006) have used the mixture model with turbulent nanofluid flow. They have shown that the mixture model can predict behaviors of nanofluid accurately.

Due to several factors such as gravity, friction between the fluid and solid particles and Brownian forces, the phenomena of Brownian diffusion, sedimentation, and dispersion may coexist in the main flow of a nanofluid. This means that the slip velocity between the fluid and particles may not be zero (Xuan and Li, 2000), therefore it seems that the two phase approach is better model to apply the nanofluid. The two phase approach is based on an assumption of continuum phases. It provides a field description of the dynamics of each phase (Eulerian–Eulerian or two fluid model) or, alternatively, the Lagrangian trajectories of individual particles coupled with the Eulerian description of the fluid flow field (Fan and Zhu, 1998; Gidaspow, 1994). One of the foremost approaches in modeling two phase slurry flow is mixture theory, also called the theory of interacting continua (Ishii, 1975; Crowe et al., 1996; Manninen et al., 1996; Xu et al., 2004). The popularity of this latter approach in multiphase applications stems from the fact that it is simple in both theory and implementation. The required computations are relatively inexpensive. Furthermore, it is straight-forward to introduce a turbulence model into the mixture model, and most of all, it is reasonably accurate for a wide range of two phase flows.

In this paper, a two phase mixture model was applied to study the laminar mixed convection of a nanofluid flow consisting of water–Al_2O_3 in a uniformly heated curved tube. Affects of magnitude of solid particles on thermal and hydrodynamic flow characters are investigated and presented.

2. Mathematical formulation

2.1. Mixture model

Laminar mixed convection of a nanofluid flow consisting of water and Al_2O_3 in a horizontal curved tube with uniform heat flux at the solid–liquid interface has been considered. Fig. 1 shows the geometry of the considered problem. The computation domain is composed of a curved circular pipe where the axial angle θ ranges from 0° to 180°, with radius a and sectional angle φ which curvature ratio δ is equal to $\frac{1}{12}$. Gravitational force is exerted in the vertical direction. The properties of the fluid are assumed constant except for the density in the body force, which varies linearly with the temperature (Boussinesq's hypothesis). Dissipation and pressure work are neglected.

The mixture model, based on a single fluid two phase approach, is employed in the simulation by assuming that the coupling between phases is strong, and particles closely follow the flow. The two phases are assumed to be interpenetrating, meaning that each phase has its own velocity vector field, and within any control volume there is a volume fraction of primary phase and also a volume fraction of the secondary phase. Instead of utilizing the governing equations of each separately, the continuity, momentum and energy equations for the mixture are employed. A nanofluid composed of water and Al_2O_3 nanoparticles flowing in a curved tube with uniform heating at the wall boundary is considered. Therefore, the dimensional equations for steady state mean conditions are as follow:

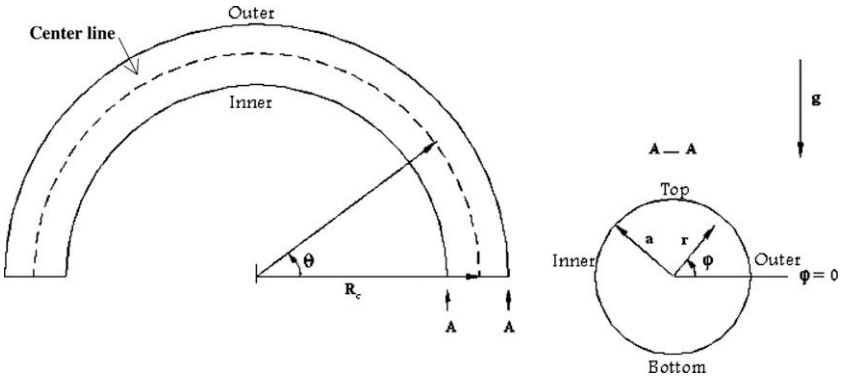

Fig. 1. Schematic of a horizontal curved tube.

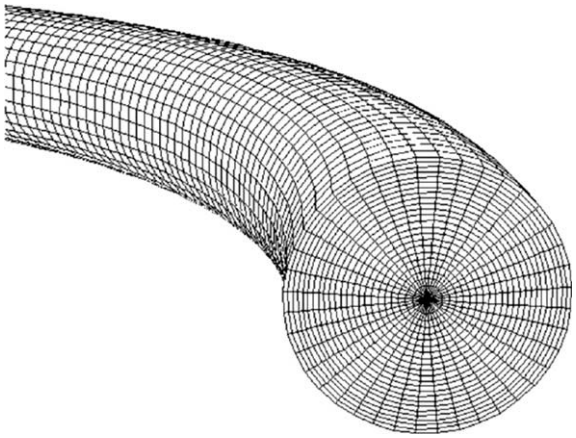

Fig. 2. Structured grid of the curved tube.

Continuity:

$$\nabla \cdot (\rho_m V_m) = 0 \tag{1}$$

Momentum:

$$\nabla \cdot (\rho_m V_m V_m) = -\nabla p + \nabla \cdot (\mu_m \nabla V_m) - \rho_{m,o} \beta g (T - T_0) + \nabla \cdot \left(\sum_{k=1}^{n} \phi_k \rho_k V_{dr,k} V_{dr,k} \right) \tag{2}$$

Energy:

$$\nabla \cdot \sum_{k=1}^{n} (\phi_k V_k (\rho_k h_k + p)) = \nabla \cdot (\lambda_m \nabla T) \tag{3}$$

Volume fraction:

$$\nabla \cdot (\phi_p \rho_p V_m) = -\nabla \cdot (\phi_p \rho_p V_{dr,p}) \tag{4}$$

ρ_m is the mixture density,

$$\rho_m = \sum_{k=1}^{n} \phi_k \rho_k \tag{5}$$

μ_m is the viscosity of the mixture that is obtained:

$$\mu_m = \sum_{k=1}^{n} \phi_k \mu_k \tag{6}$$

V_m is mass average velocity,

$$V_m = \frac{\sum_{k=1}^{n} \phi_k \rho_k V_k}{\rho_m} \tag{7}$$

λ_m is the mixture thermal conductivity coefficient,

$$\lambda_m = \sum_{k=1}^{n} \phi_k \lambda_k \tag{8}$$

An effective solid viscosity model in terms of solid volume fraction was obtained from the experimental work of Miller and Gidaspow (1992),

$$\mu_p = -0.188 + 537.42\phi \tag{9}$$

In Eq. (2), $V_{dr,k}$ is the drift velocity for the secondary phase k, i.e. the nanoparticles in the present study,

$$V_{dr,k} = V_k - V_m \tag{10}$$

The slip velocity (relative velocity) is defined as the velocity of a secondary phase (p) relative to the velocity of the primary phase (f),

$$V_{pf} = V_p - V_f \tag{11}$$

The drift velocity is related to the relative velocity,

Table 1
Grid independent test.

	Node number ($\varphi \times r \times z$)	V/V_0	T/T_0
In φ direction	$28 \times 48 \times 160$	1.2022464	1.0036362
	$40 \times 48 \times 160$	1.1849685	1.0039944
	$48 \times 48 \times 160$	1.1812318	1.0040558
In r direction	$40 \times 40 \times 160$	1.1817556	1.0042161
	$40 \times 48 \times 160$	1.1849685	1.0039944
	$40 \times 60 \times 160$	1.1874105	1.0038967
In z direction	$40 \times 48 \times 140$	1.1835162	1.0040388
	$40 \times 48 \times 160$	1.1849685	1.0039944
	$40 \times 48 \times 180$	1.1852283	1.0039705

$$V_{dr,p} = V_{pf} - \sum_{k=1}^{n} \frac{\phi_k \rho_k}{\rho_m} V_{fk} \tag{12}$$

The relative velocity is determined from Eq. (13) proposed by Manninen et al. (1996) while Eq. (14) by Schiller and Naumann (1935) is used to calculate the drag function f_{drag}

$$V_{pf} = \frac{\rho_p \, d_p^2}{18 \, \mu_f \, f_{drag}} \, \frac{(\rho_m - \rho_p)}{\rho_p} a \tag{13}$$

$$f_{drag} = 1 + 0.15 Re_p^{0.687} \tag{14}$$

The acceleration (a) in Eq. (13) is:

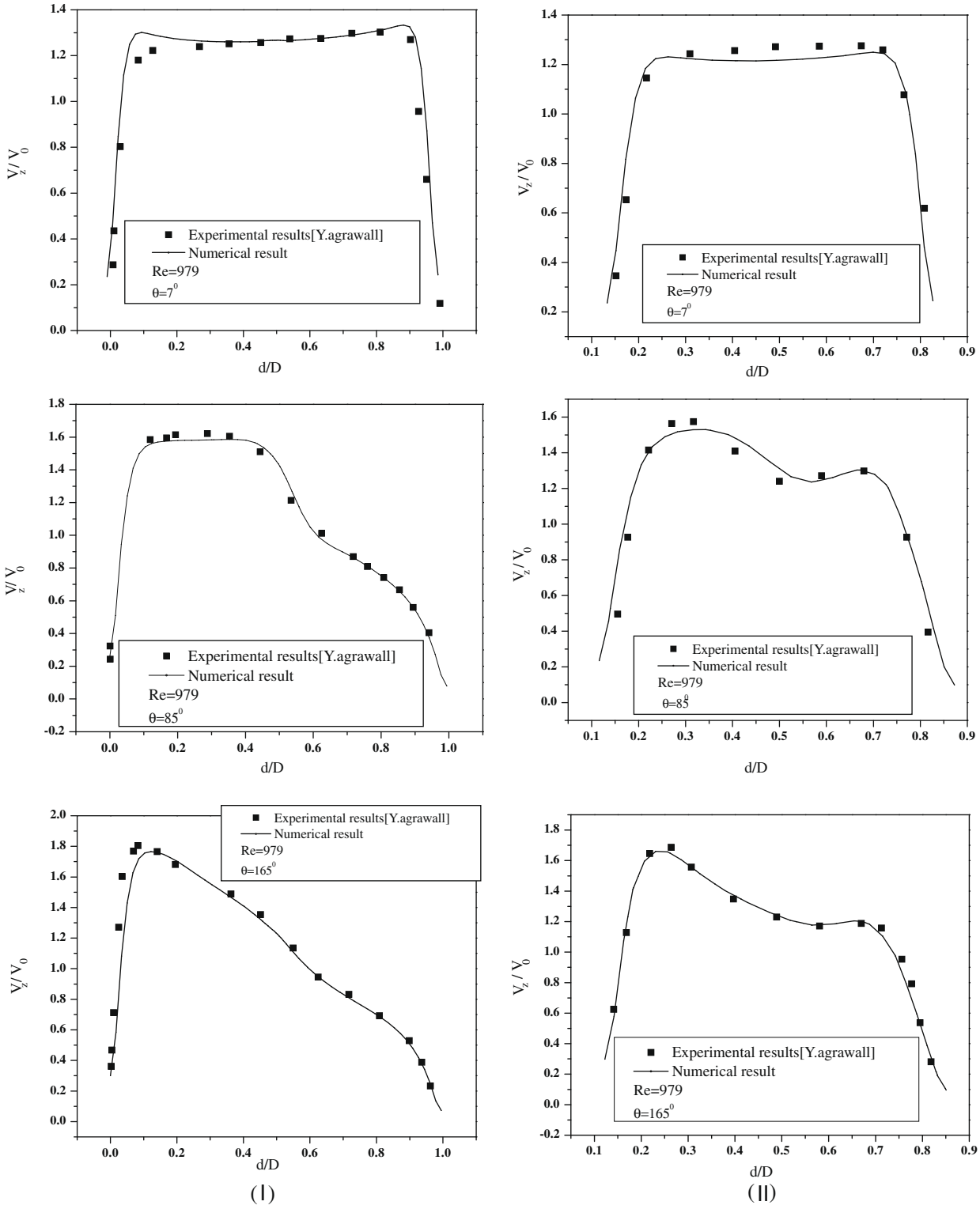

Fig. 3. Comparison of developing axial velocity profiles of fluid with pervious experimental date (Agrawal et al., 1978), (I) $\frac{y}{a} = -0.0668$ and (II) $\frac{y}{a} = -0.668$.

$$a = g - (V_m \cdot \nabla)V_m \quad (15)$$

2.2. Boundary condition

This set of coupled non-linear differential governing equations has been solved subject to following boundary conditions:

- At the tube inlet ($\theta = 0$) and $0 \leqslant r \leqslant a$:

$$V_r = 0; \quad V_\varphi = 0; \quad V_z = V_0; \quad T = T_0 \quad (16a)$$

where V_r; V_φ; V_z are radial, tangential and axial velocity respectively. Subscript 0 refer to inlet conditions and θ is angular coordinate in axial direction.

- At the fluid wall interface ($r = a$):

$$V_r = V_\varphi = V_z = 0; \quad q_w = -\lambda_m \frac{\partial T}{\partial r} \quad (16b)$$

- At the tube outlet ($\theta = 180$): the diffusion flux in the direction normal to the exit plane is assumed to be zero for all variables and an overall mass balance correction is applied.

2.3. Numerical methods

The sets of coupled non-linear differential equations were discretized using the control volume technique. A second order upwind method was used for the convective and diffusive terms while the SIMPLEC procedure was introduced to couple the velocity-pressure. A structured non-uniform grid distribution has been used to discretize the computational domain as shown in Fig. 2. It is finer near the tube entrance and near the wall where the velocity and temperature gradients are large. Several different grid distributions have been tested to ensure that the calculated results are grid independent. The selected grid for the present calculations consisted of 160, 48 and 40 nodes in the axial, radial and circumferential directions respectively. As it shows in Table 1 increasing the grid numbers does not change significantly the dimensionless velocity and temperature at the centerline region (see Table 1).

In order to demonstrate the validity and also precision of the model assumptions and the numerical analysis, calculated velocity of fluid at different axial positions is compared with the corresponding experimental results carried out by Agrawal et al. (1978) for water–glycerin at $Re = 979$. Due to adequate comparison, it is assumed that the solid volume fraction is very low. Therefore the fluid flow is solved with two phase approach then the results are validated with experimental homogenous fluid flow. As it is shown in Fig. 3 a significant agreement between the numerical and experimental results are observed at different cross sections. On the other hand, calculated local heat transfer coefficient is compared with the corresponding experimental results carried out by Wen and Ding (2004) for $Re = 1050$, $\phi = 0.01$ and $d_p = 41$ nm. In order to validate rang of the solid particles diameter, calculated velocity of particles is compared with the corresponding experimental results carried out by Lareo et al. (1997) is for $Re = 63$, $\phi = 0.3\%$ and 9 mm particles diameter. As comparison are shown in Figs. 4 and 5 a significant agreement between the calculated numerical results and reported experimental results are observed. Therefore the numerical method is reliable while it can predict the developing mixed convection flow in a horizontal curved tube with two phase approach and it can cover particles size between nanometer to millimeter.

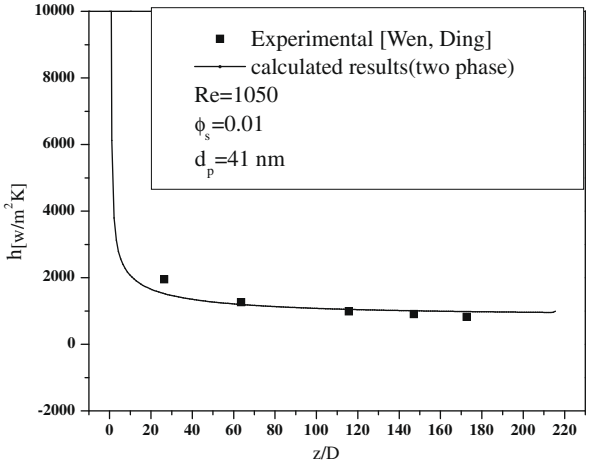

Fig. 4. Comparison of the calculated local heat transfer coefficient with pervious experimental data (Wen and Ding, 2004) at $d_p = 41$ nm.

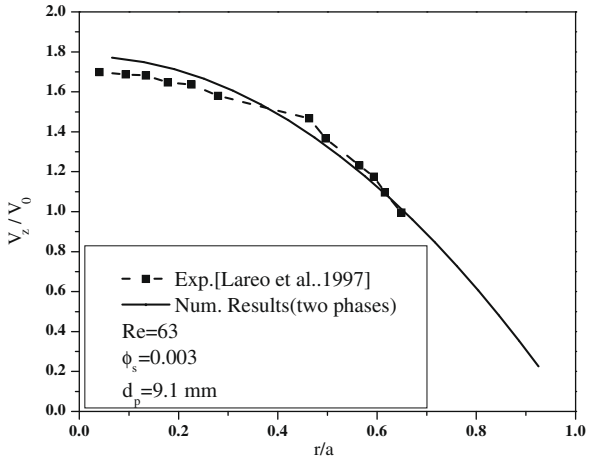

Fig. 5. Comparison of the calculated axial velocity of solid particles with pervious experimental data (Lareo et al., 1997) at $d_p = 9$ mm.

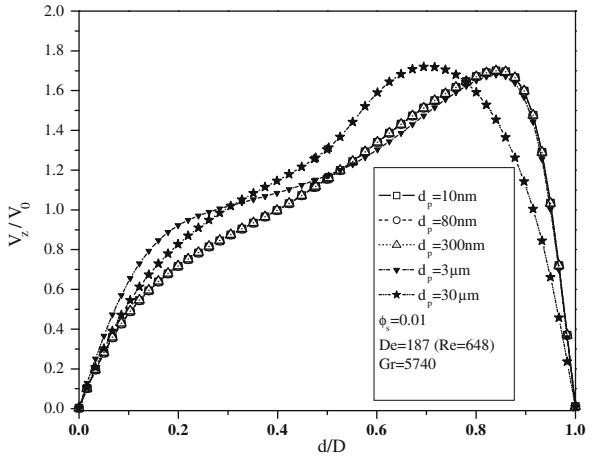

Fig. 6. Effects of the diameter of solid particles on the dimensionless axial velocity at the outlet with $De = 187$ ($Re = 648$), $Gr = 5740$, $\phi = 0.01$.

3. Results

The results are presented for nanofluid consisting water–Al_2O_3 with 0.01 solid particles concentration. Fig. 6 shows the effects of

the diameter of particles on the radial variation dimensionless axial velocity (V/V_0) at the outlet. It is shown that, increasing the diameter of particles increases the axial velocity. The variations are more significant when the diameters of particles are high. For a given De and solid particles concentration, increasing the diameter of particles augment the bulk density. Therefore the centrifugal force increases and it causes to the axial velocity augment. It is interesting to note that, increasing the diameter of particles do not have any significant effects on axial velocity, when the particles are in order of nano meter.

Fig. 7 shows that, increasing the diameter of solid particles reduces the secondary flow. Increasing the diameter of particles causes an increase in the mass of particles. Therefore, the centrifugal force and the buoyancy force can not move particles easily. Consequently, the secondary flow resulting from the centrifugal force and the buoyancy force decreases. When the diameter of particles is in order of nano meter, the secondary flow is not changed by increasing the diameter of particles.

As illustrated in Fig. 8, increasing the diameter of particles decreases the non-dimensional temperature (T/T_0). The contact surfaces between the solid particles and the base fluid decrease, also the secondary flow reduces with increasing the diameter of particles. Therefore, conductive heat transfer between flow components decreases as well as temperature in flow. The temperature is not affected by increasing the diameter of solid particles, when the particles are in order of nano meter.

The radial variations of solid particles concentration are illustrated in Fig. 9a and b. The variations in the solid particles concentration curves are very high at the outlet ($\theta = 180^\circ$), this is reason for which we show them in two figures. The solid particles concentration is uniform and constant, when the diameter of particles are in order of nano meter. In this regards the particles are not moved

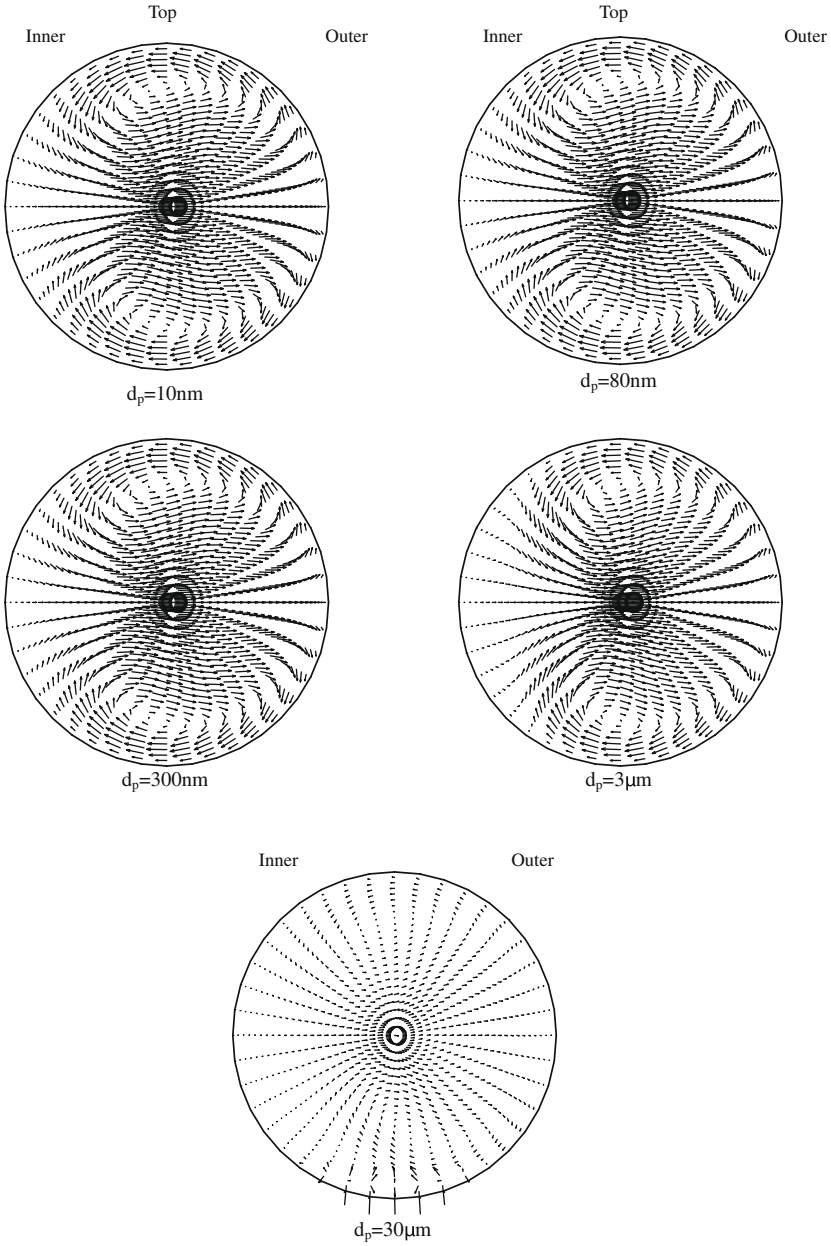

Fig. 7. The vector of non-dimensional secondary flow for various value of the solid particles diameter at the outlet with $De = 187$ ($Re = 648$), $Gr = 5740$, $\phi = 0.01$.

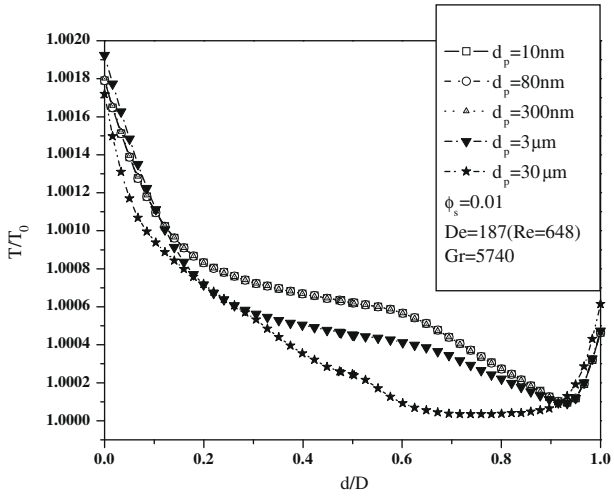

Fig. 8. Effects of the diameter of solid particles on the dimensionless temperature at the outlet with *De* = 187 (*Re* = 648), *Gr* = 5740, ϕ = 0.01.

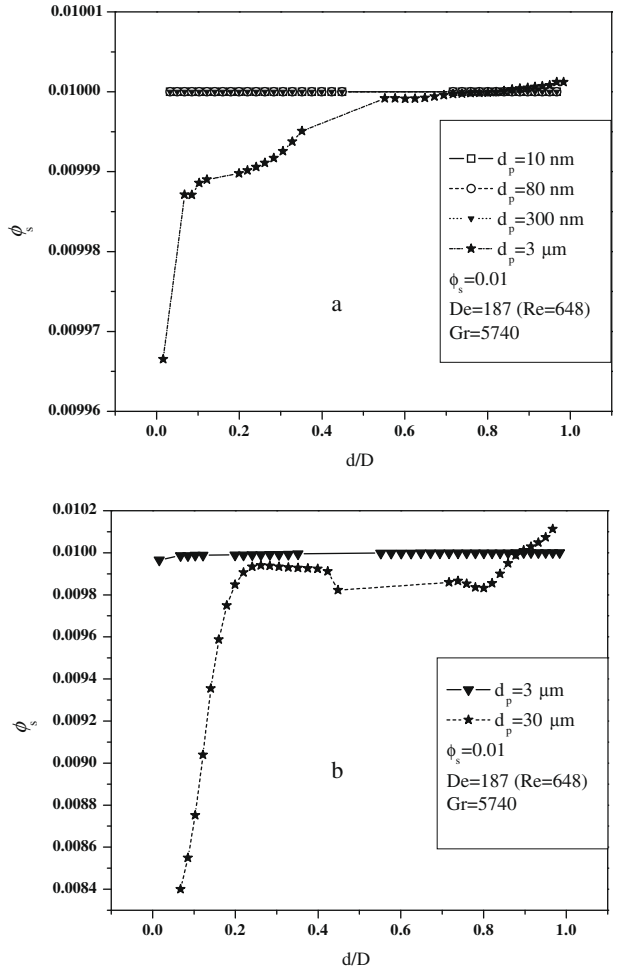

Fig. 9. Effects of the diameter of solid particles on the distribution of solid particles at the outlet with *De* = 187 (*Re* = 648), *Gr* = 5740, ϕ = 0.01.

to the outer part by the centrifugal force. This issue confirms that in the single phase approach the assumption of uniform distribution of the nanoparticles in the base flow (the homogenous flow) is correct and reliable. For higher diameter of particles, the centrif-

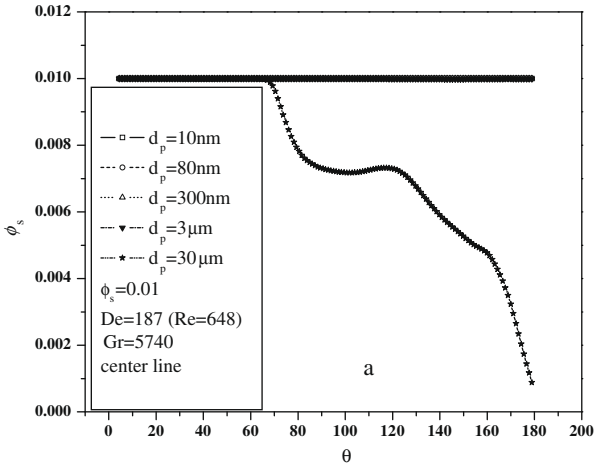

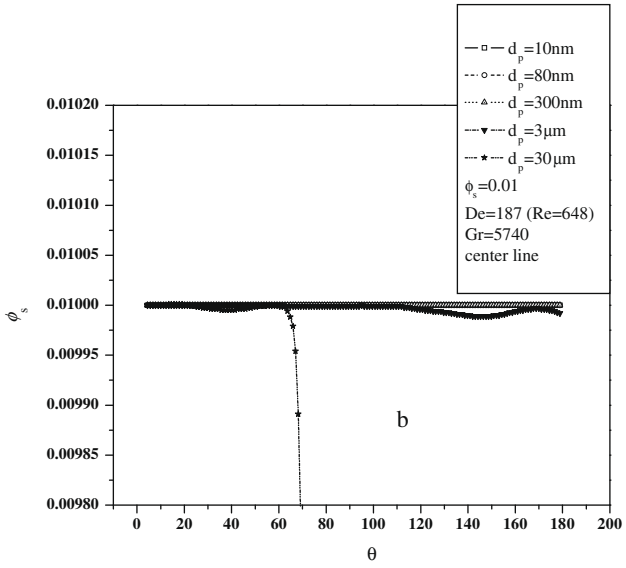

Fig. 10. The axial variation of solid particles concentration along the tube with *De* = 187 (*Re* = 648), *Gr* = 5740, ϕ = 0.01.

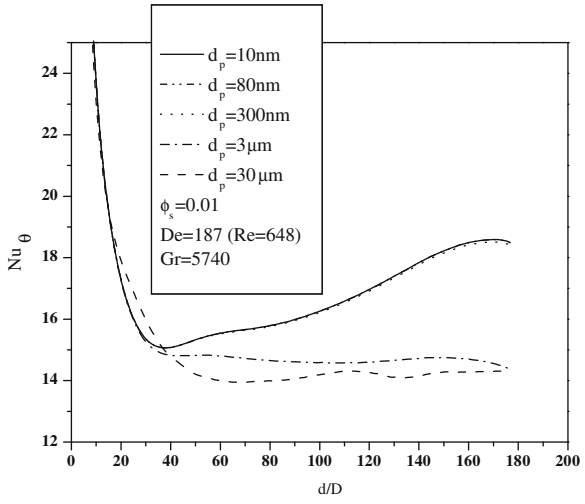

Fig. 11. Effects of the diameter of solid particles on the local Nusselt number with *De* = 187 (*Re* = 648), *Gr* = 5740, ϕ = 0.01.

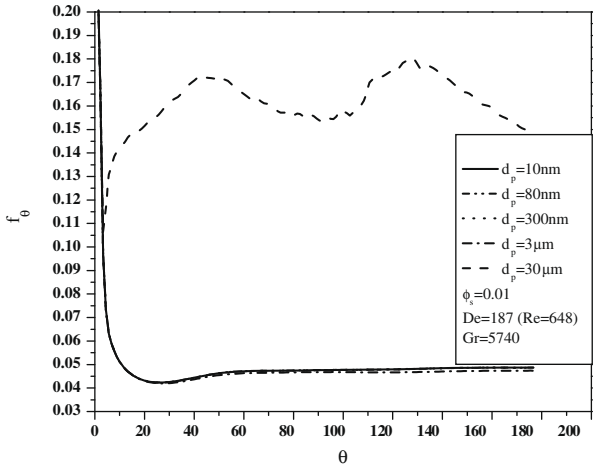

Fig. 12. Effects of the diameter of solid particles on the local skin friction coefficient with De = 187 (Re = 648), Gr = 5740, ϕ = 0.01.

ugal force causes to move particles to the outer bend. As a result, increasing the diameter of particles reduces the solid particles concentration at the inner portion. The solid particles concentration at the outer part increases because the effects of centrifugal force get stronger with increasing the diameter of particles.

The axial variation of the particles concentration is shown in Fig. 10a and b. These figures show that the centrifugal force does not change the solid particles concentration, when the diameter of particles is in order of nano meter. As a result, the distribution of nano particles is uniform and constant along the tube. Increasing the diameter of particles causes the centrifugal force stranger. Therefore, after passing $\theta = 65°$, the particles move to outer bend due to the effects of centrifugal force.

Augmenting the diameter of particles decreases the Nusselt number (see Fig. 11). The contact surface between solid particles and fluid is decreased with increasing the diameter of particles, therefore heat transfer coefficient decreases. Furthermore, increasing the diameter of particles reduces the secondary flow. Consequently, the Nusselt number along the tube reduces, particularly when the diameters of particles are order of micro meter. Increasing the diameter of particles does not have any significant effects on the Nusselt number when the diameter of particles is in order of nano meter.

The effects of diameter of particles on the skin friction coefficient are shown in Fig. 12. The skin friction reduces due to the augmentation in the diameter of particles. The skin friction is proportional to reverse velocity square. Increasing the diameter of particles augments the axial velocity (see Fig. 6), as a result skin friction decreases. But at high diameter of particles the skin friction leaps to higher value, because the contacts between solid particles and wall augment and its effects become more significant than effects of increasing axial velocity. When the diameter of particles is in order of nano meter the skin friction coefficient is not changed by increasing the diameter of particles, too.

4. Conclusions

Laminar mixed convection of a nanofluid flow consisting of water and Al_2O_3 in a circular curved tube has been studied numerically using three dimensional elliptic governing equations. Two phase mixture model and control volume technique have been implemented to study the flow field. It has been shown that for a given solid volume fraction, increasing the diameter of particles causes to augments axial velocity while the secondary flow as well as the temperature reduces. Increasing the diameter of particles decreases the Nusselt number while the skin friction augments. After passing $\theta = 65°$, the centrifugal force causes to move particles to outer bend when the particles are large, while the particles concentration is uniform and constant when the particles are in the order of nano meter. It is important that in order of nano meter (nanoparticles), increasing the diameter of particles have not any significant effect on the flow pattern. Consequence, the homogenous assumption in simulation of laminar mixed convection nanofluids flow is correct and reliable.

References

Agrawal, Y., Talbot, L., Gong, K., 1978. Laser anemometer study of flow development in curved circular pipes. J. Fluid Mech. 85 (3), 497–518.
Akbarinia, A., Behzadmehr, A., 2007. Numerical study of laminar mixed convection of a nanofluid in horizontal curved tubes. J. Appl. Thermal Eng. 27, 1327–1337.
Akbarinia, A., 2008. Impacts of nanofluid flow on skin friction factor and Nusselt number in curved tubes with constant mass flow. Int. J. Heat Fluid flow 29 (1), 229–241.
Behzadmehr, A., Saffar-Avval, M., Galanis, N., 2006. Prediction of turbulent forced convection of a nanofluid in a tube with uniform heat flux using a two phase approach. Int. J. Heat Fluid flow 28 (2), 211–219.
Choi, S.U.-S., 1995. Enhancing Thermal Conductivity of Fluids with Nanoparticles, FED Vol. 231/MD-Vol. 66. ASME Publications. pp. 99–105.
Choi, S.U.S., Zhang, Z.G., Yu, W., Lockwood, F.E., Grulke, E.A., 2001. Anomalous thermal conductivity enhancement in nanotube suspensions. Appl. Phys. Lett. 79 (14), 2252–2254.
Crowe, C.T., Troutt, T.R., Chung, J.N., 1996. Numerical models for two phase turbulent flows. Ann. Rev. Fluid Mech. 28, 11–43.
Das, S.K., Putra, N., Thiesen, P.W., Roetzel, R., 2003. Temperature dependence of thermal conductivity enhancement for nanofluids. J. Heat Transfer 125, 567–574.
Eastman, J.A., Choi, S.U.-S., Li, S., Yu, W., Thompson, L.J., 2001. Anomalously increase effective thermal conductivities of ethylene glycol based nanofluids containing copper nanoparticles. Appl. Phys. Lett. 78 (6), 718–720.
Eastman, J.A., Choi, S.U.-S., Li, S., Soyez, G., Thompson, L.J., DiMelfi, R.J., 1999. Novel thermal properties of nanostructured materials. J. Metastable Nanocryst. Mater. 2 (6), 629–634.
Fan, L.S., Zhu, C., 1998. Principle of Gas–Solid Flows. Cambridge University Press.
Gidaspow, D., 1994. Multiphase Flow and Fluidization. Academic Press.
Ishii, M., 1975. Thermo-Fluid Dynamic Theory of Two-Phase Flow. Eyrolles, Paris.
Khanfar, K., Vafai, K., Lightstone, M., 2003. Buoyancy driven heat transfer enhancement in a two dimensional enclosure utilizing nanofluids. Int. J. Heat Mass Transfer 46, 3639–3653.
Lareo, C., Branch, C.A., Fryer, P.J., 1997. Particle velocity profiles for solid–liquid food flows in vertical pipes. J. Powder Technol. 93, 23–34.
Lee, S., Choi, S.U.-S., Li, S., Eastman, J.A., 1999. Measuring thermal conductivity of fluids containing oxide nanoparticles. J. Heat Transfer 121, 280–289.
Lee, S., Choi, S.U.-S., 2000. Application of Metallic Nanoparticle Suspensions in Advanced Cooling Systems, PVP-Vol. 342/MD-Vol. 72. ASME Publication.
Li, Q., Xuan, Y., 2002. Convective heat transfer performances of fluids with nanoparticles. In: Proc. 12th Int. Heat Transfer Conference Grenoble, France, pp. 483–488.
Maige, S.E. Nguyen, C.T., Galanis, N., Roy, G., 2004a. Heat transfer enhancement in forced convection laminar tube flow by using nanofluids. ICHMT Int. Symp. Adv. Comput. Heat Transfer.
Maige, S.E., Nguyen, C.T., Galanis, N., Roy, G., 2004b. Heat transfer behaviors of nanofluids in a uniformly heated tube. Super Lattices Microstruct. 35 (3–6), 543–557.
Manninen, M., Taivassalo, V., Kallio, S., 1996. On the Mixture Model for Multiphase Flow, VTT Publications 288. Technical Research Center of Finland.
Masuda, H., Ebata, A., Teramae, K., Hishinuma, N., 1993. Alteration of thermal conductivity and viscosity of liquid by dispersing ultra-fine particles (dispersion of c-Al_2O_3, SiO_2 and TiO_2 ultra-fine particles). Netsu Bussei 4 (4), 227–233 (in Japanese).
Miller, A., Gidaspow, D., 1992. Dense, vertical gas–solid flow in a pipe. AIChE J. 38 (11), 1801–1815.
Pak, B.C., Cho, Y.I., 1998. Hydrodynamic and heat transfer study of dispersed fluids with submicron metallic oxide particles. Exp. Heat Transfer 11 (2), 151–170.
Putra, N., Roetzel, W., Das, S.K., 2003. Natural convection of nanofluids. Int. J. Heat Mass Transfer 39, 775–784.
Roy, G., Nguyen, C.T., Lajoie, P.-R., 2004. Numerical investigation of laminar flow and heat transfer in a radial flow cooling system with the use of nanofluids. Superlattices Microstruct. 35 (3–6), 497–511.
Schiller, L., Naumann, A., 1935. A drag coefficient correlation. Z. Ver.Deutsch. Ing. 77, 318–320.
Wang, X., Xu, X., Choi, S.U.-S., 1999. Thermal conductivity of nanoparticles–fluid mixture. J. Thermophys. Heat Transfer 13 (4), 474–480.
Wen, D., Ding, Y., 2004. Experimental investigation into convective heat transfer of nanofluids at the entrance region under laminar flow conditions. Int. J. Heat Mass Transfer 47, 5181–5188.

Yang, Y., Zhang, Z.G., Grulke, E.A., Anderson, W.B., Wu, G., 2005. Heat transfer properties of nanoparticle-in-fluid dispersions (nanofluids) in laminar flow. Int. J. Heat Mass Transfer 48 (6), 1107–1116.

Xue, Q.Z., 2003. Model for effective thermal conductivity of nanofluids. Phys. Lett. A 307 (5–6), 313–317.

Xu, J., Rouelle, A., Smith, K.M., Celik, D., Hussaini, M.Y., Van Sciver, S.W., 2004. Two-phase flow of solid hydrogen particles and liquid helium. Cryogenics 44, 459–466.

Xuan, Y.M., Li, Q., 2000. Heat transfer enhancement of nanofluids. Int. J. Heat Fluid Flow 21, 58–64.

Xuan, Y.M., Li, Q., Hu, W., 2003. Aggregation structure and thermal conducting of nanofluids. AIChE J. 49 (4), 1038–1043.

Xuan, Y.M., Roetzel, W., 2000. Conceptions for heat transfer correlation of nanofluids. Int. J. Heat Mass Transfer 43 (19), 3701–3707.